6. R. L. Marcialis, G. H. Rieke, L. A. Lebofsky, *Science* 237, 1349 (1987).
7. S. R. Sawyer, E. S. Barker, A. L. Cochran, W. D. Cochran, *ibid.* 238, 1560 (1987).
8. The photometric color calibrations for 4 April 1987 and 22 May 1987 were made with respect to the 1987 Primary Comparison star by using the magnitudes listed by D. J. Tholen, M. W. Buie, and C. E. Swift, [*Astron. J.* 94, 1681 (1987)].
9. Occultation events occur near rotational phase 0.75 whereas transits occur near phase 0.25, at which time Pluto's background rotational light curve displays no slope but is at a level 0.09 magnitude fainter as measured in B (*10*). It is assumed that this entire light curve variation is attributable to the rotation of surface features on Pluto and is not due to Charon (*5*). The assumption of a uniform albedo for Charon is supported by the analysis of eclipse observations (*2*).
10. R. P. Binzel and J. D. Mulholland, *Astron J.* **89**, 1759 (1984).
11. M. W. Buie and D. J. Tholen, *Bull. Amer. Astron. Soc.* **18**, 821 (1986).
12. M. V. Sykes, R. M. Cutri, L. A. Lebofsky, R. P. Binzel, *Science* **237**, 1336 (1987).
13. J. D. Muholland and B. A. Gustafson, *Astron. Astrophys.* **171**, L5 (1987).
14. D. J. Tholen and W. B. Hubbard, *ibid.*, in press.
15. This research was supported by NASA Planetary Astronomy Contract NASW 4264. The author was a guest observer at the McDonald Observatory, University of Texas. I thank Marian L. Frueh and J. Derral Mulholland for their assistance with Pluto observations during the 1987 season. This is PSI contribution number 246. The Planetary Science Institute is a division of Science Applications International Corporation.

5 April 1988; accepted 7 July 1988

Effect of a Coordination Change on the Strength of Amorphous SiO_2

CHARLES MEADE AND RAYMOND JEANLOZ

Measurements of the yield strength of SiO_2 glass to pressures as high as 81 gigapascals at room temperature show that the strength of amorphous silica decreases significantly as it is compressed to denser structures with higher coordination. Above 27 gigapascals, as the silicon in amorphous SiO_2 is continuously transformed from fourfold to sixfold coordination, the strength of the glass decreases by more than an order of magnitude. These data confirm theoretical predictions that the mechanical properties of polymerized amorphous silicates are sensitive to pressure-induced structural transformations and suggest that the viscosity of silica-rich liquids decreases significantly at high pressures. Such a change in melt rheology could enhance the processes of chemical differentiation with depth in the Earth's mantle.

On the basis of molecular dynamics simulations, Angell and co-workers (*1*) originally suggested that increases in pressure comparable to the range of values that occur in the Earth's mantle could dramatically change both the structure and viscosity of polymerized silicate melts (*2, 3*). These were important predictions because silicate melts are extremely mobile compared to crystalline rocks, and any changes in the density or viscosity of melts with depth could strongly influence the chemical differentiation and thermal evolution of the planetary interior through geologic time. In accord with the computer simulations, as well as with the interpretation of shock wave measurements on silicate melts (*4*), recent spectroscopic observations have indicated that the structures of noncrystalline silicates change markedly with pressure. Specifically, the SiO_4 tetrahedra making up the melt and glass structures at low pressures are transformed to SiO_6 octahedra (and distorted octahedra) at pressures of a few tens of gigapascals (*5*). We report measurements of the yield strength of silica glass to 81 GPa that confirm the second prediction from the molecular dynamics simulations: the mechanical properties of amorphous silicates are indeed sensitive to structural changes, such as a pressure-induced increase in coordination (*6*).

We determined the strength of amorphous silica at room temperature and high pressure by measuring the maximum shear stress supported by the glass in a diamond cell (*7–9*). We measured pressure in the samples with the ruby fluorescence technique and pressure gradients by comparing spectra from individual ruby grains distributed across the sample (*10*). The measured pressure gradient ($\partial P/\partial r$) and the sample thickness (h) closely approximate the maximum shear stress supported by the sample through the relation (*8, 9, 11*):

$$\sigma_{rz} = \frac{h\partial P}{2\partial r} \qquad (1)$$

where σ_{rz} is the shear stress acting on the plane of the diamond-sample interface and r is the radial distance from the center of the sample. The sample thickness was measured on decompressed samples at zero pressure (*12, 13*). We equate the shear stress expressed in Eq. 1 with the yield strength of the sample at high pressure (*8, 9, 11*).

All of our measurements were carried out above 8 GPa because the sample compaction is not reproducible below these pressures. At low pressures, extrusion of the sample and compaction of voids at grain boundaries control deformation. These processes occur at different rates in each sample (*14*). Also, irreversible compaction of silica glass increases the density by as much as 18% between 0 and 8 GPa (*15*), providing additional stress relaxation, which also varies between samples.

The strength of amorphous SiO_2 increases and then decreases with pressure as the glass is compressed from 8.6 to 81 GPa (Fig. 1 and Table 1). This behavior is unusual because most solids become stronger with increasing pressure and density (*8, 16*). The decrease in strength was reproducible in separate recompression experiments, which suggests that these results are independent of previous deformation and compaction (*17*). Indeed, transient effects of work hardening should not be important in the low-temperature deformation of the glass (*18*).

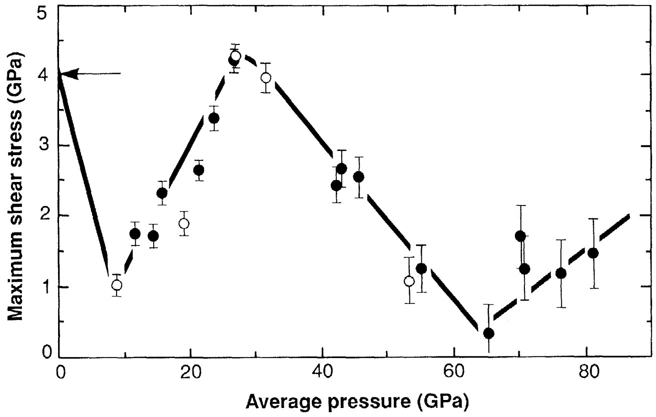

Fig. 1. Maximum shear stress in silica glass at room temperature and average pressures ($\bar{P}$) between 8.6 and 81 GPa. Each point corresponds to a separate sample, and the heavy line shows the general trend of the data. The shear stress is determined from Eq. 1, and it is a measure of the yield strength of the sample at high pressures. The error bars represent the combined uncertainties from the measurements of h and $\partial P/\partial r$. The open circles show the strength of samples that were initially compressed to 50 GPa, unloaded, and then recompressed. The arrow marks the zero pressure strength of silica glass (*19*).

Department of Geology and Geophysics, University of California, Berkeley, CA 94720.

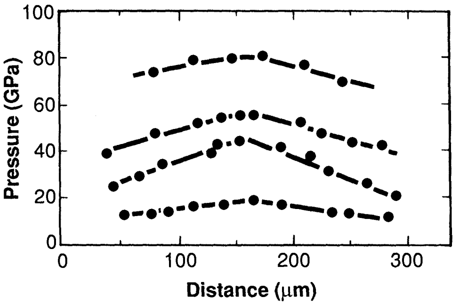

Fig. 2. Profiles of pressure gradients measured across silica glass samples at room temperature in the diamond cell. The individual points are the pressure at each radial position across the sample as determined by the ruby fluorescence technique (*10*). From low to high pressures, the average sample pressures are 13.8, 26.9, 42.1, and 76.0 GPa (Table 1).

Table 1. Summary data for SiO_2 glass.

$\bar{P}$ (GPa)	$\partial P/\partial r$ (GPa/μm)	h (μm)	σ (GPa)
11.6	0.062	56.0	1.74 (±0.15)
13.8	0.059	58.0	1.71 (±0.15)
15.6	0.080	58.0	2.32 (±0.16)
21.3	0.088	60.0	2.64 (±0.15)
23.6	0.153	44.0	3.37 (±0.16)
26.9	0.178	48.0	4.27 (±0.17)
42.1	0.130	37.0	2.41 (±0.26)
43.0	0.144	37.0	2.66 (±0.27)
45.4	0.169	30.0	2.54 (±0.28)
55.0	0.072	34.0	1.22 (±0.34)
65.0	0.018	35.0	0.32 (±0.41)
70.0	0.086	39.0	1.68 (±0.44)
70.5	0.077	37.0	1.44 (±0.44)
76.0	0.088	33.0	1.45 (±0.47)
81.0	0.072	40.0	1.44 (±0.51)
Recompressed samples			
8.6	0.028	72.0	1.01 (±0.15)
19.0	0.107	35.0	1.87 (±0.17)
27.0	0.214	40.0	4.28 (±0.17)
31.5	0.232	34.0	3.94 (±0.21)
53.0	0.073	30.0	1.10 (±0.33)

At 0 GPa the fracture strength of amorphous SiO_2 is approximately 4 GPa (*19*), whereas at 8.6 GPa the glass flows plastically and the strength is less than 1 GPa. Because the style of deformation changes from brittle to ductile over the same pressure range, the difference shown in Fig. 1 is a conservative estimate of the decrease in the creep strength of silica glass between 0 and 10 GPa (*20, 21*). This decrease in strength below 10 GPa is not produced by a change in coordination because Raman scattering (*22*) and infrared absorption (*5*) of silica in the diamond cell show that Si is tetrahedrally coordinated at these pressures. This decrease also does not reflect stress relaxation accompanying irreversible compaction because the previously compressed sample had a low strength at 8.6 GPa (*23*).

Between 27 and 62 GPa, there is another large decrease in the strength of SiO_2 glass. Linear fits to the pressure gradients across diamond cell samples (Fig. 2 and Table 1) indicate that $\partial P/\partial r$ increases sharply between average pressures of 8.6 and 26.9 GPa (*24*), but that it decreases at higher pressures. The sample thickness generally decreases with increasing pressure (Table 1), and thus the strength of the sample must also decrease above 27 GPa. Because Si in silica glass experiences a continuous increase from fourfold to sixfold coordination at approximately the same pressure (*5*), the data in Fig. 1 confirm the predictions of molecular dynamics simulations (*1*) that amorphous silicates are weakened significantly by pressure-induced coordination changes that are likely to occur inside the Earth (*25*). The recompression experiments provide additional evidence that the change in coordination is completely reversible in SiO_2 glass at room temperature. Thus, our observations of a low strength in the highly coordinated glass should be applicable to the rheology of melts because the kinetic barrier for the coordination change appears to be negligible.

We propose that the decreasing strength of SiO_2 glass above 27 GPa reflects a weakening of the Si–O bond and depolymerization of the network structure. For example, the change in coordination could increase the Si–O distance by as much as 10% (*26*) and produce a more ionic, sp^3d^2 hybridized bond (*27*). Moreover, we believe that a significant number of nonbridging oxygens are created as the SiO_4 tetrahedra are gradually compressed and distorted into a network of edge-sharing polyhedra at high pressures. Qualitatively, this model seems plausible because depolymerization significantly enhances the flow properties of silica-rich melts at low pressures (*21, 3*). In the Earth's crust, rhyolitic and dacitic magmas are particularly resistant to flow, yet with small additions of ions that depolymerize the melt structure (for example, Na^+, Al^{3+}, Mg^{2+}, Fe^{2+}, or Ca^{2+}), their viscosities can decrease by up to three orders of magnitude (*21, 28*).

That amorphous silica becomes weakened at high pressures suggests that deep in the Earth, silica-rich melts can have relatively low viscosities because their structures are depolymerized by pressure-induced coordination changes. That is, we expect that the effect of increasing pressure in the Earth's mantle is analogous to the role of network-modifying ions in silica-rich melts at low pressures. Thus, there may be substantial differences between the flow of melts in the crust and mantle. In contrast to the variability in viscosity that is readily observed in melts at the Earth's surface (*29*), the viscosity of silicate liquids may become independent of composition in the lower mantle.

REFERENCES AND NOTES

1. L. V. Woodcock, C. A. Angell, P. Cheeseman, *J. Chem. Phys.* **65**, 1565 (1976); C. A. Angell, P. Cheeseman, S. Tamaddon, *Science* **218**, 885 (1982); *Bull. Mineral* **106**, 87 (1983).
2. The calculations predict a diffusivity for the network ions. The viscosity is inversely proportional to this quantity (*3*).
3. S. Brawer, *Relaxation in Viscous Liquids and Glasses* (American Ceramic Society, Columbus, OH, 1985).
4. S. M. Rigden, T. J. Ahrens, E. M. Stolper, *Science* **226**, 1071 (1984); *J. Geophys. Res.* **93**, 367 (1988).
5. Q. Williams and R. Jeanloz, *Science* **239**, 902 (1988).
6. We measured the change in creep strength associated with a pressure-induced structural transformation in silica glass. Because creep strength and viscosity both measure the resistance to flow (at low and high temperatures, respectively), we expect that both are similarly affected by pressure-induced transformations in amorphous materials [see also J. P. Poirier, *Creep of Crystals* (Cambridge Univ. Press, Cambridge, 1985)].
7. For a complete description of the experimental methods see (*8, 9*). The samples consisted of fused silica (from Hoya Electronics), powdered to 1- to 3-μm grain size and mixed with 3% by weight ruby of similar grain size. The samples were loaded in a Mao-Bell diamond cell containing 1/5 carat diamonds with 350- or 500-μm faces; a steel gasket around the edge of the diamonds prevented the sample from extruding at the side.
8. C. Meade and R. Jeanloz, *J. Geophys. Res.* **93**, 3261 (1988).
9. C. Meade and R. Jeanloz, *ibid.*, p. 3270.
10. H. K. Mao, P. M. Bell, J. W. Shaner, D. J. Steinberg, *J. Appl. Phys.* **48**, 3276 (1978); J. D. Barnett, S. Block, G. J. Piermarini, *Rev. Sci. Instrum.* **44**, 1 (1973). The positions of the grains were determined to ±1 μm with a filar eyepiece that was calibrated against a precision graticule.
11. C. M. Sung, C. Goetze, H. K. Mao, *Rev. Sci. Instrum.* **48**, 1386 (1977).
12. The thickness was measured to ±1 μm by focusing a microscope on the upper and lower faces of the recovered samples. In previous studies on crystalline materials (*8, 9*), we have corrected the zero-pressure measurements to the elastically compressed values at pressure by using the known equations of state of the sample materials. The pressure-volume relation for fused silica, however, is poorly constrained at room temperature and high pressure ($P > 10$ GPa). The reversible elastic compression has been measured between 0 and 10 GPa (*13*); above 10 GPa, the glass is irreversibly compacted, and thus the "elastic" compression is difficult to measure. Hugoniot measurements do not necessarily constrain the room temperature, quasi-static equation of state that is pertinent to this study, and the glass may transform to stishovite at large shock compressions [G. A. Lyzenga, T. J. Ahrens, A. C. Mitchell, *J. Geophys. Res.* **88**, 2431 (1983); R. G. McQueen, J. N. Fritz, S. P. Marsh, *J. Appl. Phys.* **33**, 922 (1962)]. Therefore, we have calculated the shear stress in Eq. 1 on the basis of measurements of the sample thickness after decompression to 0 GPa. We estimate that decompression from the highest pressures produces linear strains of no more than 12%, and thus the shear stresses in Fig. 2 may be an overestimate of the yield strength by up to a similar amount. This results in an uncertainty that is small compared to the total experimental error at 80 GPa. More importantly, it tends to yield an underestimate of the decrease in yield strength at high pressure.
13. C. Meade and R. Jeanloz, *Phys. Rev. B* **35**, 236 (1987).
14. Because the gasket is not compressed between the diamond faces (*7, 8*), it does not influence the strength of the sample. Previous experiments (*8*) and the reproducibility of the present data show that strength is independent of gasket material and sample size.

15. J. D. Mackenzie, *J. Am. Ceram. Soc.* **46**, 461 (1963); J. Arndt and D. Stöffler, *Phys. Chem. Glasses* **10**, 117 (1969).
16. P. W. Bridgman, *Proc. Am. Acad. Arts Sci.* **71**, 387 (1937).
17. In the recompression experiments, samples were initially loaded to 50 GPa, decompressed to 0 GPa, and then recompressed to high pressures.
18. In contrast, work hardening can increase the yield strength by more than a factor of 2 in crystalline materials with a limited number of slip systems [H. C. Heard, in *Flow and Fracture of Rocks*, H. C. Heard *et al.*, Eds. (American Geophysical Union, Washington, DC, 1972), pp. 191–209].
19. B. A. Proctor, I. Whitney, J. W. Johnson, *Proc. R. Soc. London Ser. A* **297**, 534 (1967).
20. At 0 GPa, silica glass fractures because the critical stress for nucleating and extending cracks is less than the critical stress for moving defects and dislocations. Thus the ductile creep strength must be greater than 4 GPa at room pressure and temperature. Extrapolations of experimental data suggest that the viscosity of silica glass is greater than 10^{30} Pa·s at 0 GPa and 300 K [W. Primak, *J. Appl. Phys.* **55**, 852 (1984); see also (*21*)]. These extrapolations provide an upper bound on the change in creep strength at room temperature; they imply that the time scale for viscous deformation decreases by 18 orders of magnitude between 0 and 10 GPa.
21. G. Urbain, Y. Bottinga, P. Richet, *Geochim. Cosmochim. Acta* **46**, 1061 (1982).
22. R. Hemley *et al.*, *Phys. Rev. Lett.* **57**, 547 (1986).
23. In previous experiments (*13*), we measured plastic flow in individual glass fragments under shear stresses of ~0.1 GPa at 10 GPa confining pressure. This value compares well with the results in Fig. 1, and it shows that the low strength at ~10 GPa is not due to grain boundary sliding in our samples.
24. The shape of a diamond cell sample resembles a thin disk. If the pressure gradient is measured outward from the center over a distance, *r*, the average pressure ($\bar{P}$) over that interval occurs at the point $r/\sqrt{2} = 0.707r$ from the center.
25. The observations of (*5*) have been interpreted as a range of Si coordinations distributed between four and six at 39 GPa, the highest pressure of their study. The strength data suggest that tetrahedral coordination may persist up to 60 GPa at 300 K.
26. This value is the average increase in Si–O distance in crystalline silicates between tetrahedral and octahedral structures. We compared bond lengths between α-quartz [L. Levien, C. T. Prewitt, D. J. Weidner, *Am. Mineral* **65**, 920 (1980)] and stishovite [W. Sinclair and A. E. Ringwood, *Nature* **272**, 714 (1978)] and between enstatite [N. Morimoto and K. Koto, *Z. Kristallogr.* **129**, 65 (1969)] and $MgSiO_3$ perovskite [E. Ito and Y. Matsui, *Earth Planet. Sci. Lett.* **38**, 443 (1978); T. Yagi, H. K. Mao, P. M. Bell, *Phys. Chem. Minerals* **3**, 97 (1978)].
27. M. A. Spackman, R. J. Hill, G. V. Gibbs, *Phys. Chem. Minerals* **14**, 139 (1987).
28. T. Murase, A. R. McBirney, *Geol. Soc. Am. Bull.* **84**, 3563 (1973).
29. Whereas eruptions of silica-rich magmas produce steep cinder cones, silica-poor melts form broad shield volcanoes and continental flood basalts [*Basaltic Volcanism Study Project* (Pergamon, New York, 1981)].
30. We thank H. K. Mao and Q. Williams for helpful discussions and two anonymous reviewers for helpful comments on an earlier manuscript. This work was supported by the National Science Foundation. R.J. thanks the Fairchild scholar program at the California Institute of Technology for partial support.

4 May 1988; accepted 18 July 1988

Mitotic Recombination Within the Centromere of a Yeast Chromosome

SUSAN W. LIEBMAN,* LORRAINE S. SYMINGTON,† THOMAS D. PETES‡

Centromeres are the structural elements of eukaryotic chromosomes that hold sister chromatids together and to which spindle tubules connect during cell division. Centromeres have been shown to suppress meiotic recombination in some systems. In this study yeast strains genetically marked within and flanking a centromere, were used to demonstrate that gene conversion (nonreciprocal recombination) tracts in mitosis can enter into and extend through the centromere.

CENTROMERIC DNA FORMS A TIGHT complex with proteins that is very resistant in vitro to nuclease digestion (*1*). One might expect that recombination could not occur within such a protein-DNA complex. Indeed, in *Drosophila*, meiotic recombination near the centromere is greatly suppressed (*2*). However, in yeast, we found that meiotic conversion tracts frequently span the centromere (*3*). We also found that meiotic conversion occurs at approximately normal rates near the centromere. In contrast, Lambie and Roeder (*4*) suggested that the yeast centromere represses meiotic conversion about fivefold. These different findings on the effect of the centromere on the rates of meiotic conversion may reflect differences in genetic background or the types of constructions used.

Mitotic gene mapping in yeast is based on the frequency of crossovers between genes and their centromeres. The original presumption (*5*) was that in mitosis, duplicated sister chromatids were held together by their centromeres while they recombined with their nonsister homologs. Consequently, the further a gene was from its centromere, the greater the chance of a crossover uncoupling sister alleles from the same centromere. Thus, about half the time, depending on the segregation of the homologous chromosomes, mitotic crossing-over will lead to heterozygous markers distal to the crossover becoming homozygous.

Recent evidence (*6*–*8*) suggests that a considerable portion of mitotic recombination occurs prior to chromosome duplication. The two-strand–stage model of recombination (*6*) suggests that crossovers occur in G_1 between homologous DNA single strands of the same polarity and are resolved

Table 1. Numbers and types of presumptive convertants derived from SLP-6 and S-5 parent strains. Standard genetic procedures for yeast were used to score for markers and to determine mating types (*22*). Trichodermin (TCM) resistance was scored on nonselective media containing 0.20 mg of the drug per milliliter. Trichodermin was stored as a 20 mg of solution in 50% ethanol at −20°C. The pluses and minuses indicate the growth of the strains on media lacking Leu, Ura, His, or Thr or the presence or absence of the Xho I or Nru I restriction sites. NA means not applicable. Representative presumptive α/α and **a**/**a** strains were shown to be diploid because the viability of meiotic progeny after crossing to diploid mating-type homozygous testers was good, while bad spore viability (characteristic of a triploid) was obtained when they were crossed to haploid testers. As expected genetic tests indicated that all heterozygous markers not on chromosome III remained heterozygous in the SLP-6 convertants. Numbers in heading state the number of convertants obtained.

Marker	SLP-6						S-5					
	ura3⁻						*ura3⁻*			Tcm resistance		
	21	1	2	1	1	2	2	2	2	5	10	4
Leu	+	−	+	+	−	+	+	+	−	+	+	−
Ura	−	−	−	−	−	−	−	−	−	+	−	−
Xho I	+/−	+/−	−/−	−/−	−/−	−/−	+/−	+/+	+/+	+/+	+/+	+/+
Nru I	+/−	+/−	+/−	+/+	+/+	+/+	NA	NA	NA	NA	NA	NA
His	NA	NA	NA	NA	NA	NA	+	−	−	−	−	−
Thr	NA	NA	NA	NA	NA	NA	+	+	+	+	+	+
MAT	α/**a**	α/**a**	α/**a**	α/**a**	α/**a**	α/α	α/**a**	α/**a**	**a**/**a**	α/**a**	α/**a**	**a**/**a**

Department of Molecular Genetics and Cell Biology, University of Chicago, Chicago, IL 60637.

*On sabbatical leave from the Laboratory for Cellular Molecular and Developmental Biology, Department of Biological Sciences, University of Illinois at Chicago, Box 4348, Chicago, IL 60680.

†Present address: Institute of Cancer Research, College of Physicians and Surgeons of Columbia University, New York, NY 10032.

‡Present address: Department of Biology, University of North Carolina, Chapel Hill, NC 27599.